

# Bonding Properties of Aluminum Alloy Plate and Concrete

Haoran Wang

Guangxi Huaxin Sheng Civil Engineering Technology Co., Ltd; wanghaoran@whioce.com

**Abstract:** Aluminum alloy material has the advantages of high strength, good deformation performance, corrosion resistance, etc. it is an ideal material for steel reinforced concrete structure reinforcement engineering in coastal erosion environment. The cohesive property of aluminum alloy plate and concrete is the key problem whether the aluminum alloy plate and steel bar concrete beam can work together. Based on this, the bonding performance between aluminum alloy plate and concrete is tested and theoretically studied. Considering the influence of strength of mixed concrete, width and thickness of aluminum alloy plate, bonding length and interface treatment on the bonding performance of aluminum alloy plate and concrete block, a set of specimen fixing device was designed, and 105 bonded specimens of aluminum alloy plate and mixed concrete prism were tested in-plane single shear by universal testing machine. According to the test results and theoretical analysis, the typical characteristics of cohesive failure, shear stress distribution curve and cohesive slip curve of aluminum alloy plate and mixed concrete are obtained. The research shows that there are two types of failure of the specimen: interfacial peeling failure and mixed concrete layer peeling failure. Interface treatment has an important influence on the bonding performance. The specimens without roughening the bonding interface have interface peeling and breaking, while other specimens have concrete layer peeling and breaking. As the strength of the mixed concrete increases and the width and thickness of the aluminum alloy plate decrease, the cohesiveness can be improved. There is an effective adhesive length. When the adhesive length is greater than the effective adhesive length, increasing the adhesive length does not increase the ultimate load of the connection.

**Keywords:** Aluminum alloy plate; Adhesion property; In-plane single shear test; Shear stress; Stripping failure

## 1. Introduction

Aluminum alloy material has high specific strength (its density is 2,700 kg/m<sup>3</sup>, about 1/3 of that of steel material; the strength is high, the strength of aluminum alloy 6061-T6 used for structural reinforcement is 210-250 MPa, which is equivalent to the strength of Q235 steel, corrosion resistance, good deformation performance (the extreme deformation is greater than 10%), and mechanical properties of strength and ductility that do not drop but rise in low temperature environment. The reinforcement of reinforced concrete beams with aluminum alloy plates can meet the special needs of reinforcement projects in coastal erosion environment, humidity, low temperature, high cold and other extreme environments. Compared with current common materials for reinforcing reinforced concrete beams, aluminum alloy has obvious advantages: its deformation performance is better than FRP and corrosion resistance is better than steel plate. Before the project, a trial study was carried out on aluminum alloy plate and steel reinforced concrete beams, Rasheed et al., Abdalla et al., Obeidah et al., LiuHongbin and Tuguigang, and a finite element analysis was carried out on Song Qixi and Abu-Obeidah et al. The above research shows that aluminum alloy plate is obviously superior to CFRP plate in ductility at the same time of significantly improving and fixing the bearing capacity of reinforced concrete beams. The bonding property between aluminum alloy plate and concrete is the key to whether aluminum alloy plate and steel reinforced concrete beam can work together. Before the end, the research on the cohesive property of mixed concrete mainly focused on FRP and steel plates, while the research on the cohesive property of aluminum alloy plates and mixed concrete is

still blank. Because aluminum alloy plates have different material properties and surface characteristics from these sheets, it is necessary to study the cohesive properties of aluminum alloy plates and mixed concrete. Based on this, in-plane single shear tests of 105 bonded specimens of aluminum alloy plate and concrete prism were carried out. According to the test results, combined with theoretical analysis, the failure characteristics of the specimen, the load-displacement relationship of the bond, the distribution rule of shear stress, the effective bond length and the bond-slip characteristics are obtained.

## 2. Test Plan

### 2.1 Test Design

Acetone is used to clean the connection interface between the roughened (or non-roughened) aluminum alloy plate and the concrete prism. After the interface is dry, the structural adhesive prepared according to the comparative example is evenly applied to the adhesion range of the aluminum alloy plate, with the thickness of the adhesive layer being about 3 mm. Then, the aluminum alloy plate is adhered to the surface of the concrete prism body to form a single shear test specimen for the adhesion performance of the aluminum alloy plate and the concrete prism body, as shown in fig. 1. In fig. 1, the ABCD portion of the aluminum alloy plate is divided into adhesive regions, and its length AC is shown by  $l_a$ . The CE part of the protruding prism body is 150 mm long and is used for the clamp of the testing machine to load the test piece along the axial direction of the aluminum alloy plate.

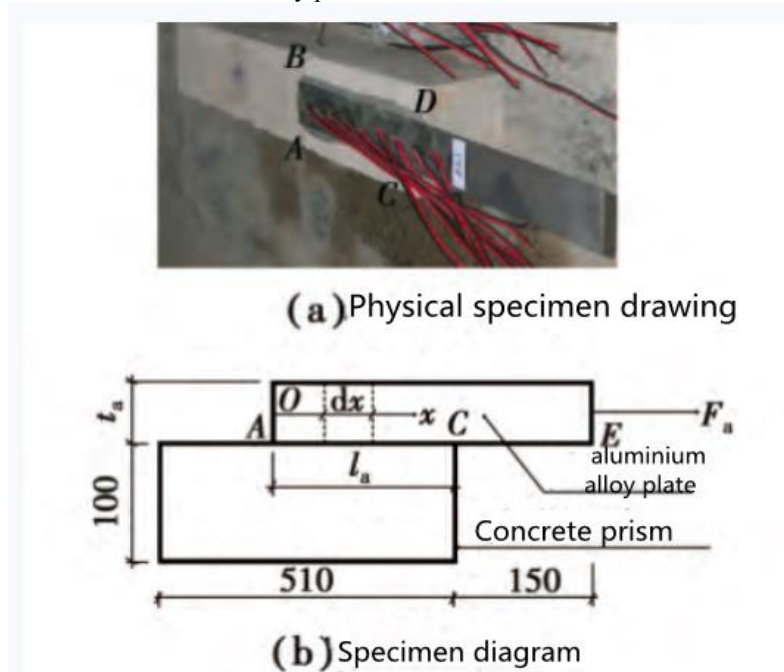


**Figure 1;** The specimen of in – plane simple shear test

The aluminum alloy plate is 6061-T6 aluminum alloy plate produced by Guangxi south-south aluminum co., ltd. the plate width  $b_a$  is 45 mm and 30 mm, and the plate thickness  $t_a$  is 4 mm and 2 mm. The structural adhesive is JN structural adhesive produced by the limited public company and developed by the local wood technology in Kurt Bong, South Lake. The concrete prism is cast with commercial mixed concrete produced by the limited public company in Nanning Huarun Xixiangtang concrete, with a size of 100 mm× 100 mm× 510 mm [16].

There are four kinds of interface treatment methods for the specimens, which are respectively represented by A, B, C and D, namely: A is concrete roughening and aluminum alloy plate roughening; B is the roughening of mixed concrete, and the aluminum alloy plate is not roughened; C is mixed concrete without chipping, aluminum alloy plate roughening; D is that concrete is not roughened and aluminum alloy plates are not roughened.

The test pieces are divided into 5 groups, and a group of comparison groups (group II) is set up. The boundary surface

treatment (group I), mixed concrete strength (group III), aluminum alloy plate width (group IV) and plate thickness (group V) of the comparison groups are separately changed. The cohesive property of the test pieces is compared with that of the comparison groups to investigate the influence of boundary surface treatment, concrete strength, aluminum alloy plate width and thickness and other factors on the cohesive property. In groups II to V, each group has only 8 specimens with different bonding lengths, and the bonding lengths are respectively 25, 50, 75, ..., 200 mm to investigate the effect of bonding length on the bonding properties of aluminum alloy plates and concrete blocks. In-plane single shear test specimen parameters are shown in Table 1. In order to eliminate the accidental and discrete effects of the test, all the test pieces are designed with 3 identical test pieces, so there are altogether 5 groups of 105 test pieces. The experiment was completed in the laboratory of the School of Civil and Architectural Engineering of Guangxi University.

No.	MIT	$f_{cu}$	$b_a/$ mm	$t_a/$ mm	$l_a/$ mm	No.	MIT	$f_{cu}$	$b_a/$ mm	$t_a/$ mm	$l_a/$ mm
I-1	B	C35	45	4	150	III-8	A	C20	45	4	200
I-2	C	C35	45	4	150	IV-1	A	C35	30	4	25
I-3	D	C35	45	4	150	IV-2	A	C35	30	4	50
II-1	A	C35	45	4	25	IV-3	A	C35	30	4	75
II-2	A	C35	45	4	50	IV-4	A	C35	30	4	100
II-3	A	C35	45	4	75	IV-5	A	C35	30	4	125
II-4	A	C35	45	4	100	IV-6	A	C35	30	4	150
II-5	A	C35	45	4	125	IV-7	A	C35	30	4	175
II-6	A	C35	45	4	150	IV-8	A	C35	30	4	200
II-7	A	C35	45	4	175	V-1	A	C35	45	2	25
II-8	A	C35	45	4	200	V-2	A	C35	45	2	50
III-1	A	C20	45	4	25	V-3	A	C35	45	2	75
III-2	A	C20	45	4	50	V-4	A	C35	45	2	100
III-3	A	C20	45	4	75	V-5	A	C35	45	2	125
III-4	A	C20	45	4	100	V-6	A	C35	45	2	150
III-5	A	C20	45	4	125	V-7	A	C35	45	2	175
III-6	A	C20	45	4	150	V-8	A	C35	45	2	200
III-7	A	C20	45	4	175						

**Table 1;** Details of the specimens of in-plane simple shear test

Note: no. Indicates the serial number of the test piece; MIT (Models of Interfacial Treatment) indicates the interface processing method.

## 2.2 Test Equipment and Loading System

A set of mounting for fixing the test piece is designed, and its material is Q235 steel. As shown in Figure 2, WAW-600 micro-machine controlled electro-hydraulic servo universal testing machine is used to load the test piece. The loading mounting is shown in Figure 3. The installation and installation diagram of the test piece is shown in fig. 4. During the test, the test piece is placed between the upper and lower horizontal steel plates of the device. The aluminum alloy plate CD extends close to the left plate wall of the upper horizontal steel plate cavity. Tighten the bolts on the four vertical screws to compress the concrete prism. Then, the test piece fixing device is placed between the upper and lower clamps of the testing machine, and the lower clamp of the testing machine is used to anchor and fix the installed vertical steel plate of the test piece, and the upper clamp clamps the ce part of the aluminum alloy plate. Since the center of the upper and lower clamps of the testing machine, the vertical steel plate and the aluminum alloy plate are located on the same vertical plane, the axial tension of the aluminum alloy plate and the in-plane shear force of the test piece are ensured.

The upper fixture is used to apply axial tensile force to the aluminum alloy plate, and the loading degree is controlled by position shift, with the loading rate of 0.5%. 2 mm/min, single adjustment loading, when the specimen peeling failure to stop loading.

The outer surface of the aluminum alloy plate connected with the concrete area (i.e. ABCD part in fig. 1) is axially provided with strain gauges. When the adhesion length  $l_a = 25$  mm, the strain gauge spacing is 12.5 mm, a total of 3 should change piece; when the sticking length  $l_a = 50 \sim 200$  mm, the spacing between strain gages is 25 mm, totaling  $(l_a/25+1)$  strain gages. The strain gauge shall be numbered from the loading end (i.e. CD), and the strain gauge shall be arranged as shown in fig. 5. After the test piece is installed in place on the test machine, the shorter end of the l-shaped steel piece is pasted on the aluminum alloy plate with 502 glue water to extend out of the fixed installation part (ce) of the test piece. The longer end is 5 mm away from the horizontal steel plate, and a displacement sensor is installed on it to test the axial displacement of the aluminum alloy plate on CD, as shown in fig. 4. Strain and displacement signals pass through DH 3821 static stress strain testing system, and load signals pass through testing machine micro-machine control system for automatic collection and storage.



Figure 2; Specimen Fixing Device



Figure 3; Loading Device

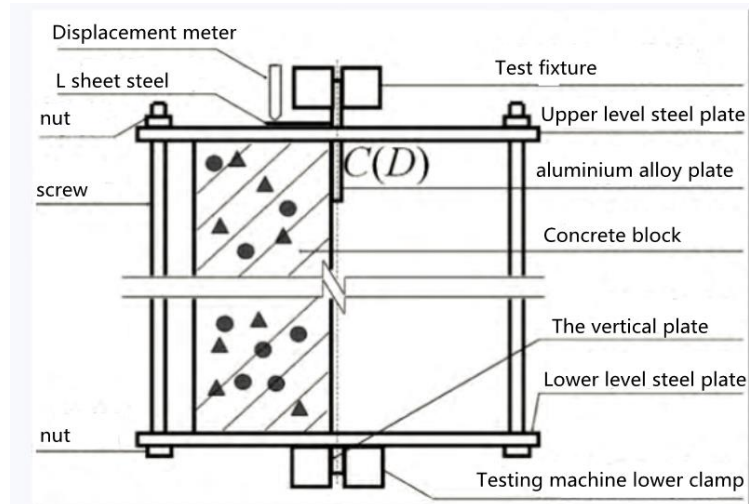


Figure 4; the specimen installation

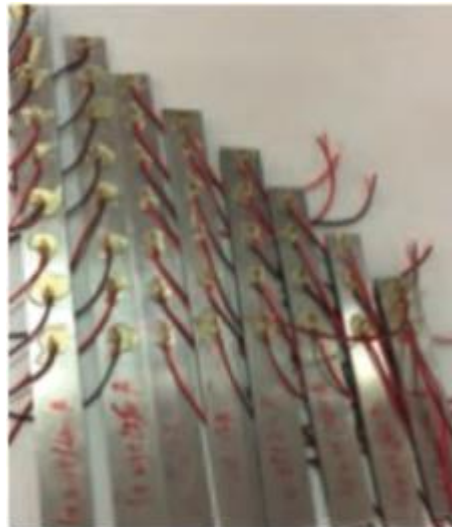


Figure 5; The layout of schematic diagram

### 2.3 Material Mechanical Properties

According to the report provided by the manufacturer, the mechanical properties of the structural adhesive are shown in Table 2. In table 2:  $f_{pt}$  is tensile strength;  $F_{pm}$  is bending strength;  $F_{pc}$  is the compressive strength;  $E_p$  is elastic modulus;  $\epsilon_{pu}$  is elongation.

Table 2 Mechanical Properties of Structural Adhesive

$f_{pt}/\text{MPa}$	$f_{pm}/\text{MPa}$	$f_{pc}/\text{MPa}$	$E_p/\text{GPa}$	$\epsilon_{pu}/\%$
36	65	92	6.1	1.8

Concrete prism and concrete cube standard test blocks were cured under standard conditions for 28 days. According to the Standard of Test Methods for Mechanical Properties of Ordinary Concrete (GB/T 50081-2016), Hualong Concrete Pressure Tester was used to carry out compressive tests on concrete cube standard test blocks. The test results are:  $f_{cu} = 26.8 \text{ MPa}$  (C20),  $f_{cu} = 41.3 \text{ MPa}$  (C35).

According to "Metallic Materials Tensile Test Part 1: Room Temperature Test Method" (GB/T 228. 1-2010), the tensile test was carried out on the aluminum alloy plate tested by MTS 809Axis/Torsional Test System. The rectangular tensile specimen of aluminum alloy plate is shown in fig. 6, and the mechanical performance index is shown in table 3. In Table 3:  $E_A$  is the elastic modulus of aluminum alloy at the origin;  $f_{0.1}$  and  $f_{0.2}$  is the residual strain of 0 respectively. 1% and 0.2% of the corresponding stress;  $f_{au}$  is the ultimate strength of aluminum alloy.  $\epsilon_{au}$  is the ultimate strain;  $n$  is a parameter representing the constitutive relation of aluminum alloy material (as shown in formula (3)).

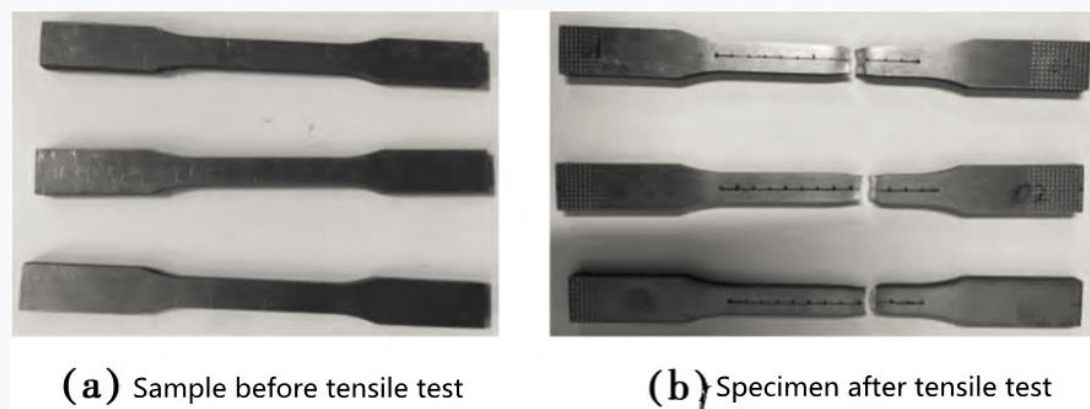


Figure 6; Rectangular Tensile Specimen of Aluminum Alloy Plate

Specimen number	$E_a /$ MPa	$f_{0.1} /$ MPa	$f_{0.2} /$ MPa	$f_{au} /$ MPa	$f_{0.2} /$ $f_{0.1}$	$\epsilon_{au} /$ $\mu\epsilon$	$n$
6061-1	71 941.3	245.8	265.3	314.77	1.079	101 000	9.12
6061-2	66 756.4	258.6	275.0	314.58	1.063	105 000	11.35
6061-3	68 301.1	250.7	271.5	313.77	1.083	104 753	8.69
The average	68 999.6	251.7	270.6	314.37	1.075	103 584	9.72

Table 3; Mechanical Properties of Aluminum Alloy Plate

### 3. Test Results and Analysis

#### 3.1 Stripping Failure Mode

Before the failure of the specimen, there was no obvious relative deformation between the aluminum alloy plate and the concrete block. After hearing the crackling sound of the two, the relative deformation increased abruptly, and then the aluminum alloy plate and the concrete block peeled off, causing the specimen to undergo peeling failure. There are two types of stripping failure, namely:

1) Interface peeling failure: the interface treatment is a failure mode of components of b, c and d; the failure occurred at the interface of aluminum alloy plate or mixed concrete, and there was no obvious friction dent and no residual structural adhesive at the failure interface. There is no crack in the concrete, and the bond load and relative displacement at the time of failure are less than that of the concrete layer stripped from the damaged specimen. The reason for the failure

is that when the interface is not roughened, the adhesion force between the boundary surface and the structural adhesive is less than the tensile strength of the mixed concrete, and the interface of the structural adhesive aluminum alloy plate (or concrete) becomes a weak link. Because the aluminum alloy plate is smoother than the concrete surface, when the aluminum alloy plate is not roughened (regardless of whether the mixed concrete boundary surface is ground, i.e. the boundary surfaces of b and d are arranged in a square way), the interface of the aluminum alloy plate with the generated structural adhesive is peeled off and broken, as shown in fig. 7 (a). When the aluminum alloy plate is roughened and the concrete is not polished (i.e. the interface treatment method is c), the bound surface of the coagulated soil with the generated binder is peeled off and broken, as shown in fig. 7 (b). The interfacial debonding failure is not allowed to occur during reinforcement. Therefore, the interface must be roughened to enhance the bonding load between the interface and the adhesive layer.

2) Concrete layer peeling failure: the interface treatment is the failure mode of component a. When the interface treatment is broken, the structural adhesive adhered to the aluminum alloy plate will tear off the mixed concrete within 5 mm of the surface layer of the mixed concrete boundary surface and remain on the aluminum alloy plate. The failure interface is uneven and belongs to concrete tensile failure, as shown in fig. 7 (c). Stripping failure of concrete layer is a form of failure recommended by "Code for Design of Concrete Structure Reinforcement" (GB 50367-2013), which proves the suitability of aluminum alloy plate for consolidation of mixed concrete structure.



Figure 7; Stripping Failure Form

### 3.2 Bond Load Displacement Curve

The ultimate bond loads of 105 specimens in 5 groups measured by in-plane single shear test are shown in Table 4. It can be seen from the table that although there are some differences in the extreme bonding loads of the three specimens, the difference is not very large. The biggest difference between the ultimate bond load of the specimen and its flat value is the first specimen of I-3, which is 10%, and the error difference of other specimens is between-9.14%~8. Between 84%.

The average value  $f_a$  of the bonding loads of the three specimens with the same number is taken as the ordinate, and the average value  $s$  of the axial displacement of the aluminum alloy plate at CD is taken as the horizontal coordinate, thus making the bending line of the bonding load displacement of the specimens.

No.	1	2	3	$F_a$	No.	1	2	3	$F_a$	No.	1	2	3	$F_a$
I-1	6.40	5.81	6.08	6.10	III-2	5.07	4.84	4.94	4.95	IV-6	9.28	8.39	8.79	8.82
I-2	6.81	7.09	6.96	6.95	III-3	6.99	6.39	6.67	6.68	IV-7	9.31	9.43	9.37	9.37
I-3	6.38	5.27	5.74	5.80	III-1	8.50	9.05	8.78	8.78	IV-8	9.31	9.52	9.42	9.42
II-1	3.44	3.58	3.51	3.51	III-5	9.61	8.85	9.22	9.23	V-1	2.59	2.96	2.75	2.77
II-2	6.30	5.48	5.84	5.87	III-6	10.31	10.34	10.33	10.33	V-2	4.53	4.96	4.73	4.74
II-3	8.57	7.40	7.93	7.97	III-7	10.60	10.66	10.63	10.63	V-3	5.83	6.00	5.92	5.92
II-1	10.27	9.81	10.03	10.04	III-8	10.61	11.49	11.02	11.04	V-4	6.50	7.46	6.92	6.96
II-5	11.38	13.22	12.19	12.26	IV-1	2.68	2.53	2.60	2.60	V-5	6.59	6.66	6.63	6.63
II-6	11.91	11.99	11.94	11.95	IV-2	4.91	4.38	4.62	4.64	V-6	6.59	6.73	6.66	6.66
II-7	11.95	12.12	12.04	12.04	IV-3	6.68	6.03	6.33	6.35	V-7	6.59	6.60	6.58	6.59
II-8	11.95	12.26	12.11	12.11	IV-4	8.00	6.75	7.30	7.35	V-8	6.59	6.60	6.58	6.59
III-1	2.74	2.78	2.75	2.76	IV-5	8.86	9.21	9.04	9.04					

**Table 4; Ultimate Bond Load Test Results**

Note: 1, 2 and 3 are the ultimate bond loads of 3 specimens with the same number respectively;  $F_a$  is the average value of ultimate bond load of specimens with the same number.

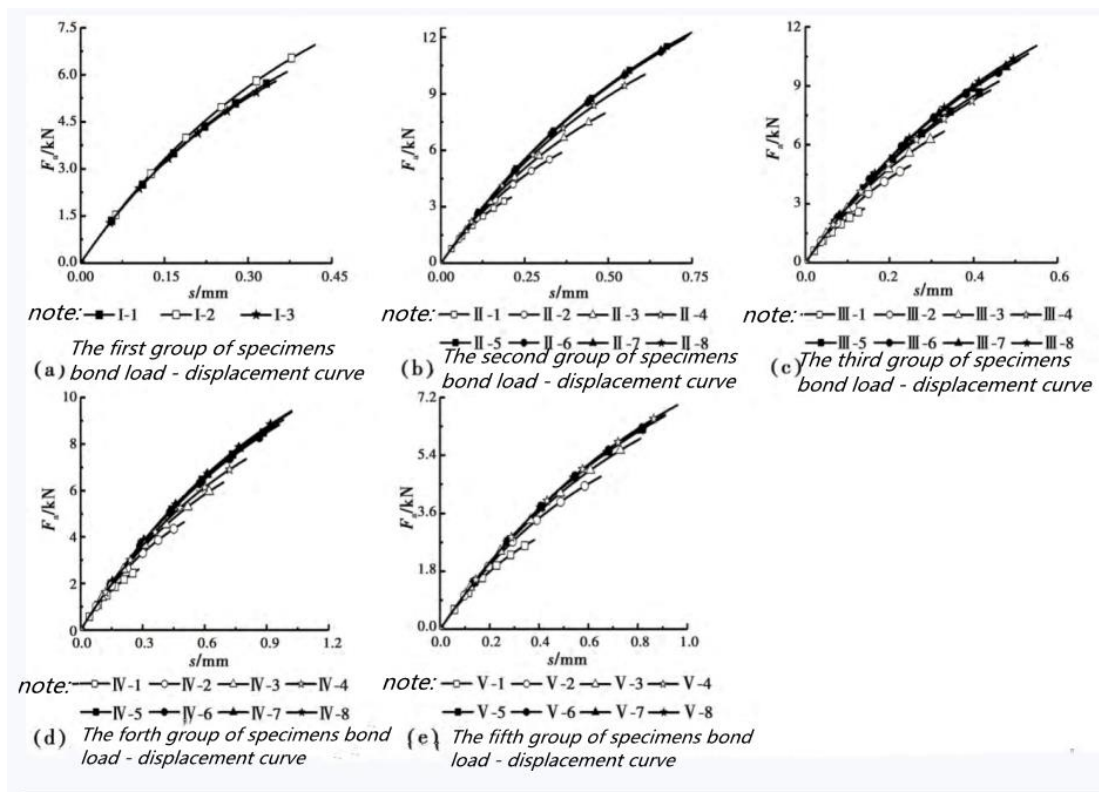


Figure 8 Bond Load Displacement Curve of Specimen

As can be seen from fig. 8 and table 4:

1) As the load increases, the slope of curve gradually decreases due to the accumulation of damages. From loading to failure, the specimen basically has no plastic deformation, and the displacement of the plate end is very small, less than 1 mm during failure.

2) With the increase of adhesive length, the load of the extremely limited adhesive junction increases. However, when the bonding length is increased to a certain value, the extreme bonding load will not be increased. This shows that there is an effective bonding length between aluminum alloy plate and concrete. When the effective bonding length is exceeded, increasing the bonding length will not increase the ultimate bonding load of the specimen.

### 3.3 Shear Stress Distribution Curve

The aluminum alloy plate element with  $dx$  length is taken from fig. 1 (b), as shown in fig. 9. Let the thickness of aluminum alloy



plate be  $t_a$ , the width be  $b_a$ , the normal stress be  $\sigma_a$ , the normal strain be  $\epsilon_a$ , and the bond shear stress be  $\tau$ . establish an equilibrium equation along the x-direction. There are

$$b_a t_a (\sigma_a + d\sigma_a) = b_a t_a \sigma_a - \tau b_a dx \quad (1)$$

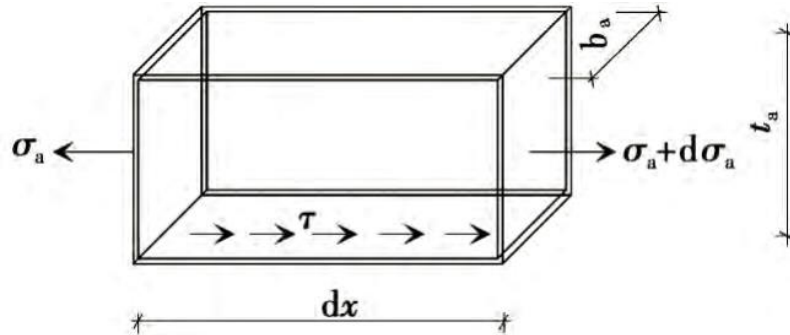


Figure 9; Stress Analysis Diagram of Specimen

Available by Formula (1)

$$\tau = - t_a \frac{d\sigma_a}{dx} \quad (2)$$

The constitutive relation of aluminum alloy material is

$$\epsilon_a = \frac{\sigma_a}{E_a} + 0.002 \left( \frac{\sigma_a}{f_{0.2}} \right)^n \quad (3)$$

The aluminum alloy plate at this point measured by strain gauge shall be changed  $\epsilon_a$ . I Substitution formula (3), to obtain the corresponding  $\sigma_{a,i}$ , followed by formula (2) to obtain the bonding shear stress at each point

$$\tau_i = - t_a \frac{\sigma_{a,i} - \sigma_{a,i+1}}{\Delta_{i,i+1}} \quad (4)$$

In formula (4),  $\Delta_{i,i+1}$  is the spacing between the I-th and I+1-th changeable sheets, I is taken from the beginning of 1, and the maximum value is 9, which is taken when  $l_a = 200$  mm. It should be pointed out that equation (4) obtains the average interfacial shear stress between adjacent strain gauges, ignoring the influence of aluminum alloy plate thickness, and its precision is related to the gauge spacing and aluminum alloy plate thickness. Fig. 10 shows the distribution curve of shear stress  $\tau$  along the sticking length of some specimens. in the figure, x refers to the distance from the loading end (CD in fig. 1), and shear stress  $\tau$  is the average value of three specimens with the same number. As can be seen from fig. 10:

1) The interface shear stress is in an inverted "U" shape with large middle to small two ends. The CD interface shear stress at the loading end is zero (where the normal stress of aluminum alloy plate is the largest), and the maximum shear stress appears on the side near the loading end. When the load is small, the occurrence position is about 25 mm. As the cohesive load  $f_a$  increases, the initial damage accumulation and stress redistribution occur due to the appearance of fine microcracks on the surface of the mixed concrete. The maximum shear stress moves slightly from the end ab, and its occurrence distance is not more than 75 mm from the loading end.

2) As the adhesive load  $F_A$  increases, the length of the structural adhesive participating in shear increases. When the load is greater than 60% of the extreme adhesive load  $F_{Ab}$ , the length of the structural adhesive participating in shear no longer increases with the increase of the adhesive load  $F_A$ , but remains at a certain value. Since the bonding length  $l_a$  of the structural adhesive is greater than

the effective bonding length  $l_e$ , the shear stress  $\tau$  of the boundary surface outside the effective bonding length  $l_e$  on the free end side is equal to zero, and the effective bonding length has nothing to do with the actual bonding length.

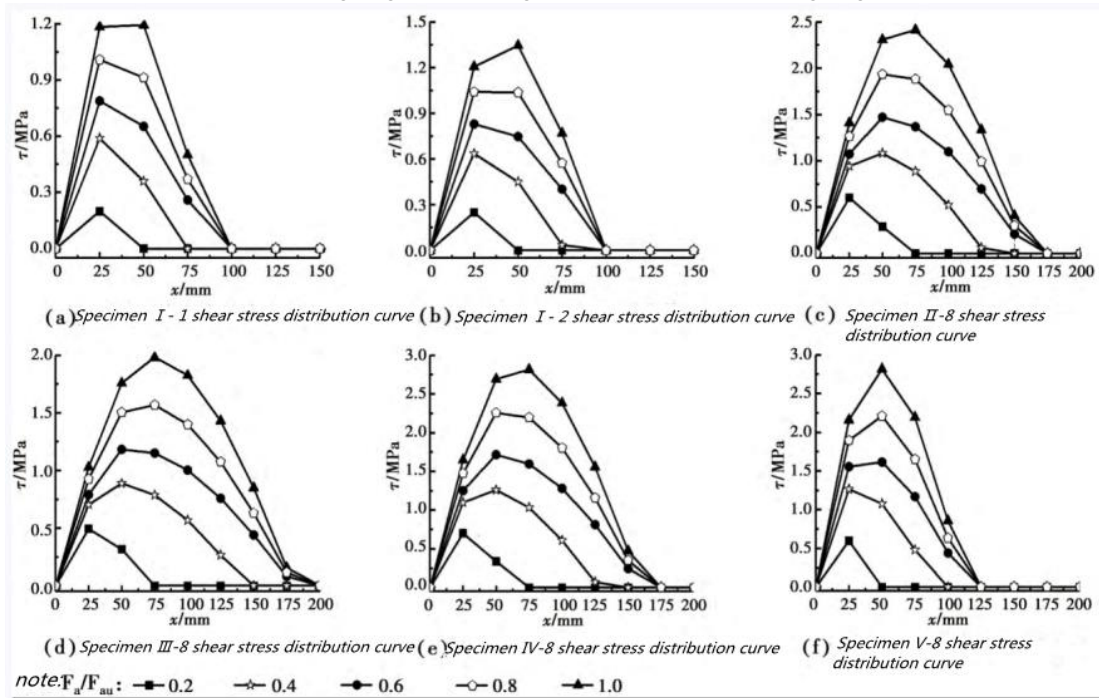


Figure 10; Shear Stress Distribution Curve of Specimen

Analyzing fig. 10, we can get the influence

1) The influence of interface management. The differences between test piece I-1, test piece I-2 and test piece ii-8 are different at the boundary surface (since the adhesive length is greater than the effective adhesive length, the difference in adhesive length will not affect the mechanical performance of the test piece). As can be seen from figs. 10 (a) to 10 (c), the maximum shear stress of test piece I-2 is slightly larger than that of test piece I-1, which indicates that the surface of bright and smooth aluminum alloy plate has a greater impact on cohesive energy than mixed concrete. The maximum shear stress of specimens I-1 and I-2 is less than 1.3 MPa, 100 mm from the loading end shear stress is equal to zero; the maximum shear stress of specimen II-8 is 2.4 MPa left and right, the shear stress 175 mm from the loading end is equal to zero; the effective bonding length and maximum shear stress of specimens I-1 and I-2 are both smaller than those of specimens II-8. The maximum shear stress at the interface is related to the roughness of the surface of concrete and aluminum alloy plate materials. The coarser and rougher the surface of the material, the greater the cementation, friction and mechanical engagement with the adhesive layer, and the greater the maximum shear stress. The smooth interface greatly reduces the maximum shear stress that the connection can bear, which affects the stress redistribution of the adhesive layer. Its load transfer capacity phase should be weakened, and the effective adhesion length phase should be reduced. It can be seen that the interface must be roughened before pasting aluminum alloy plates to increase the connection bearing capacity.

2) The influence of the strength of mixed concrete. Specimen II-8 and Specimen III-8 differ only in concrete strength. As can be seen from figs. 10 (c) to 10 (d), the maximum shear stress of test piece ii-8 (C30 mixed concrete) is larger and the effective sticking length is smaller than that of test piece iii-8 (c25 mixed concrete). In the test, the specimens with interface treatment method A all suffered from spalling failure of mixed solidified soil. At the initial stage of loading, a crack parallel to the boundary surface appeared in the mixed solidified soil with a thickness of several millimeters under the structural adhesive at the loading end. With the increase of the cohesive load, the structural adhesive developed from the loading end to the free end. When the load increased to the ultimate cohesive load, the mixed solidified soil with the same surface was peeled off from the mixed solidified soil mass by the aluminum alloy plate. Therefore, the maximum shear stress is closely related to the tensile strength of mixed concrete. The greater the tensile strength of mixed concrete,

the greater the maximum shear stress it can bear. The effective sticking length of specimen III-8 is relatively large, which indicates that the load transfer and stress redistribution of structural adhesive can be ensured as long as the interface is roughened.

3) Influence of aluminum alloy plate width. Test piece II-8 and test piece IV-8 differ only in width of aluminum alloy plate. As can be seen from figs. 10 (c) and 10 (e), the maximum shear stress of test piece ii-8 ( $b_a = 45$  mm) is smaller than that of test piece iv-8 ( $b_a = 30$  mm), and the effective sticking length is unchanged. The influence of aluminum alloy plate width on the connection bearing capacity is reflected in the constraint of surrounding concrete on the connection. The smaller the width of aluminum alloy plate, the greater the constraint of unit aluminum alloy plate by surrounding concrete, and the greater the corresponding bonding load.

4) Influence of aluminum alloy plate thickness. Sample II-8 and Sample V-8 differ only in thickness of aluminum alloy plate. As can be seen from figs. 10 (c) and 10 (f), the maximum shear stress of test piece ii-8 ( $t_a = 4$  mm) is smaller than that of test piece v-8 ( $t_a = 2$  mm), and the difference in effective sticking length is not shown in the figure (because the distance between strain gauges is 25 mm, the difference less than 25 mm may not be shown).

### 3.4 Bond Slip Curve

The slip  $s_i$  at the  $i$  strain gauge is

$$s_i = s_{i-1} - \frac{\epsilon_{a,i} + \epsilon_{a,i-1}}{2} \Delta_{i,i+1} \quad (5)$$

$s_1$  is equal to the loading end displacement, measured by the loading end displacement meter. In this way, the bond slip curve with different positions of each test piece can be obtained from equations (4) and (5). The shear stress  $\tau_i$  and sliding movement  $s_i$  respectively take the average value of three specimens with the same serial number to obtain the bond-slip curve of each specimen. As shown in Figure 11, 25 mm and 50 mm in the legend refer to the distance from the loading end CD.

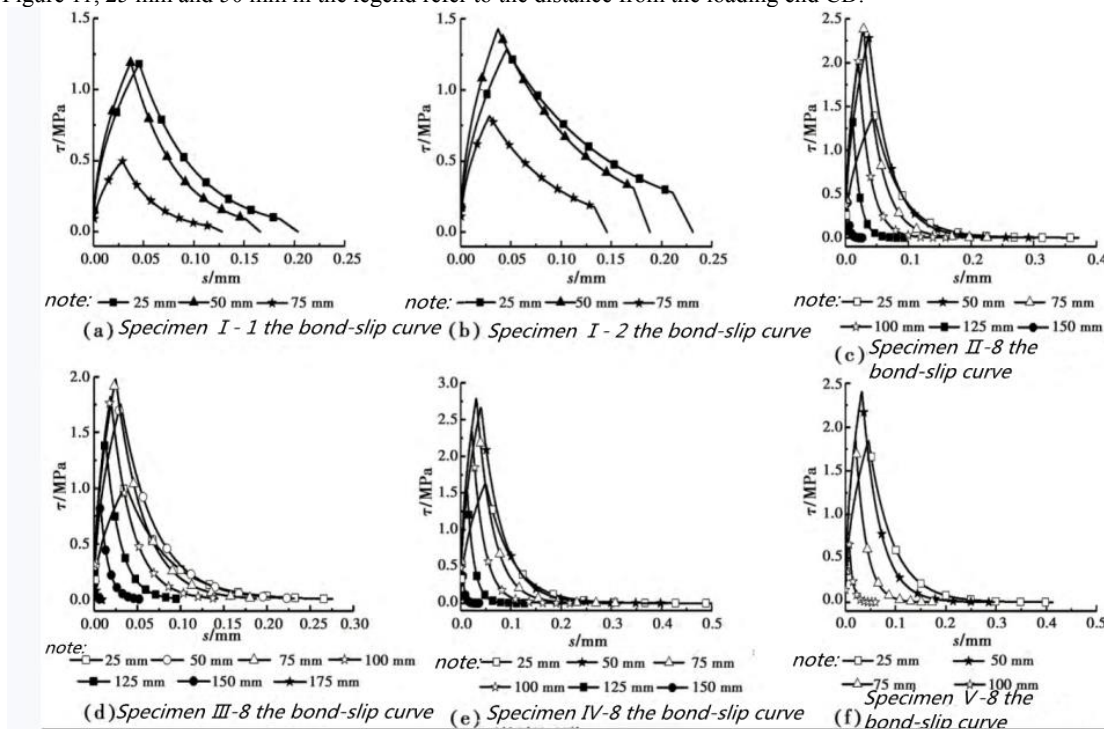


Figure 11; Bond Slip Curve

As can be seen from fig. 11, the sticky knot sliding curve has the following characteristics:

1) The bond-slip curve has an ascending section and a descending section. The sliding movement in the ascending section of the curve is very small, and most of the partial sliding movement is completed in the descending section. In the descending section, the curve approaches to the horizontal axis as the slip increases.

2) When the shear stress approaches the limit shear stress, the slope of the cut line of the curve becomes smaller, the slope of the tangent line at the origin of the curve is the largest, and the slope of the cut line at the apex is the smallest. This is because the specimen is in the elastic stage at the origin, and the process from shear stress to ultimate shear stress is the process of concrete crack occurrence and development, the process from elastic state to plastic state, the process of damage accumulation, and the corresponding process of interface stiffness reduction.

3) Specimen I-1 and specimen I-2 are interfacial debonding failures. In addition to the specimen characteristics that the maximum shear stress and limit displacement are smaller than that of concrete layer debonding failures, their bond-slip curves also have different characteristics. In the descending section, due to sliding movement at the boundary surface, their shear stress suddenly drops to zero, which is even more sudden.

4) The surface area enclosed by the bonding slip curve and the transverse setting mark indicates the interface fracture energy of the connection. The greater the interface fracture energy, the better the bearing capacity of the connection. The same conclusion can also be drawn from the angle of the interfacial fracture energy. as can be seen from fig. 11, the interfacial fracture energy of test piece I-1 is the smallest, and the interfacial fracture energy of test piece iv-8 is the largest.

## 4. Conclusion

The bonding property between aluminum alloy plate and concrete is an important factor affecting the reinforcement effect. In order to solve this problem, a set of testing and fixing device has been set up in our company. Five groups of 105 specimens of aluminum alloy plate and mixed concrete prism connected body have been subjected to in-plane single shear test, and the following conclusions have been obtained:

1) There are two failure modes of the specimen: interface stripping failure and mixed soil layer stripping failure.

2) The interface treatment has an important influence on the cohesiveness. When the mixed concrete is not roughened or the aluminum alloy plate is not roughened, the interface peeling failure occurs, and its cohesiveness is poor. Therefore, the interface must be roughened or roughened.

3) The interfacial shear stress presents an inverted "U" shape distribution with large middle and small two ends. The interfacial shear stress at the loading end is zero, and the maximum shear stress appears about 25 mm near the loading end. With the increase of bond load, the maximum shear stress moves slightly toward the free end, and its occurrence distance is not more than 75 mm from the loaded end.

4) As the strength of concrete increases and the width and thickness of aluminum alloy plates decrease, the bonding performance increases.

5) In the test, the shear stress of the specimen is not zero and the length from the loading end is not more than 175 mm, which indicates that there is an effective bonding length. When the bonding length is greater than the effective bonding length, increasing the bonding length cannot improve the ultimate load of the connection.

## References

1. Xing Guohua, Xie Pengyu, Song Qixi, et al. Research on the Mechanical Properties of Aluminum Alloy Reinforced Concrete Beams Strengthened with External Prestressing Force [J]. *Silicate Bulletin*, 2016,35 (3): 831-836.
2. Liu Hongbin. Theoretical and Experimental Study on Failure Mode of Mixed Concrete Beam with Aluminum Alloy and Steel Reinforcement [D]. Harbin: Harbin Institute of Technology, 2011.
3. Tu Guigang. Experimental study and numerical analysis of aluminum alloy reinforced steel reinforced concrete beams [D]. Harbin: Harbin Institute of Technology, 2011.
4. Song Qixi. Study on Mechanical Properties of Aluminum Alloy Reinforced Concrete Beams with External Prestressing Force and Solidification [D]. Xi 'an: Chang 'an University, 2015.